JOURNAL OF NATURAL REMEDIES
DOI: 10.18311/jnr/2025/45866
RESEARCH ARTICLE

Development and Formulation Optimization of Plumbagin Loaded Niosomes for MCF-7 Breast Cancer

Jyoti K. Jawale[1*], Vrushali S. Kashikar[1,2], Shashikant N. Dhole[1] and Sonali R. Devne[1]

[1]Department of Pharmaceutics, Savitribai Phule Pune University, PES Modern College of Pharmacy (For Ladies), Pimpri Chinchwad – 412105, Maharashtra, India; jyotijawale364@gmail.com
[2]Department of Pharmaceutics, Amepurva Forum, Solapur – 413002, Maharashtra, India

Abstract

Background: Plumbagin encounters several biopharmaceutical hurdles that impede its medical use, including low aqueous solubilization, high lipophilic characteristics, instability from spontaneous sublimation, and poor oral bioavailability. These issues considerably limit its therapeutic effectiveness. In addition, plumbagin struggles to achieve therapeutic concentrations in tumors due to its lack of tumor-targeting ability and fast clearance from the body. To attain effective treatment levels, high or frequent dosing is necessary, which often leads to adverse side effects such as diarrhea, skin irritation, elevated white blood cell counts, and increased neutrophil levels. **Aim:** This study aimed to formulate plumbagin-loaded niosomes utilizing Span 60 as the non-ionic surfactant, combined with cholesterol. **Method:** The reverse phase evaporation methodology was used to create niosomal formulations. Particulate size, Polydispersity Index (PDI), and zeta potential were assessed through optical scattering analysis. **Result:** The result was shown an average particle size from 84.5± 5.85 nm to 123.5± 4.82nm. The Zeta potential value was found to be -26.8 ± 2.13 mv and both percent entrapment efficiency and release rate were evaluated by UV spectroscopy. % EE was found 91.42 ± 2.19. %. *In vitro* drug release, niosomes were shown sustain release behavior as compared to pure plumbagin. *In vitro* cytotoxicity assay was conducted to assess antitumor potential on MCF-7 cell lines. Ultimately, the MTT test revealed that plumbagin loaded niosomes exhibit an enhanced cytotoxic action on MCF-7 cell as in contrast to plumbagin alone. **Conclusion:** The result demonstrated that biopharmaceutical properties of naturally derived phytochemicals can be increased by loading it into niosomes, thus enhance their anticancer efficacy.

Major Findings: The Plumbagin loaded niosomes shown potent anticancer activity on MCF-7 Breast cancer cell as compared to cisplatin and free plumbagin, this might be due to increased cellular uptake, and sustained release of Plumbagin niosomes, leading to prolonged interaction with cancer cells.

Keywords: Niosomes, Plumbagin, Release Rate, Reverse Phase Evaporation, Tumour Targeting

1. Introduction

Millions of people die from cancer each year, making it the most deadly disease in the world. It is the most significant health problem of the 21st century, affecting individuals from all backgrounds and cultures. Unchecked cell division followed by the absence of apoptosis is what defines cancer. There are limitations and negative effects connected with every cancer therapy strategy that has been implemented. Surgical removal, chemotherapy, hormone therapy, and radiation are some of these treatment approaches. Chemotherapy's side effects involve the destruction of healthy cells, particularly in the bone marrow, digestive system, hair follicles, and macrophages, leading to significant collateral damage alongside its cancer-fighting effects. The chemotherapeutic drugs that are now in use can cause anemia, thrombocytopenia, alopecia, and organ malfunction. Because of these adverse effects, anticancer medication may be stopped, dose reduced,

*Author for correspondence

Article Received on: 15.09.2024 Revised on: 25.11.2024 Accepted on: 03.12.2024

or treatment delayed, which results in less favorable clinical outcomes from the chemotherapy[1-3].

Chemotherapeutic drugs early removal from the systemic circulation is a significant disadvantage as well. Another aspect lowering the possibility for biological membrane penetration of anticancer medicines is their lower solubility in water. Additionally, the surfaces of malignant cells over express P-glycoprotein, a multidrug resistance protein that functions as an efflux pump to stop drugs from building up inside tumors[4]. Dense tumors may not respond to chemotherapy because cell division may essentially halt in the tumor's core. Moreover, chemotherapy drugs frequently fail to enter solid tumors and destroy the malignant cells within because they cannot reach the tumor's core[5].

Increased concentrations of anticancer medications can be delivered to tumors specifically to improve cancer treatment. This will raise the drug therapeutic efficiency against malignant cells while minimizing negative effects on healthy tissues. The nanoscale length ranges from 1 to 100 nm, where particles are small enough to create new features through quantum effects and electron confinement. Because of their distinct quantum mechanical origin, materials in the form of nanoparticles display distinctive properties from their larger counterparts[6]. At the moment, nanomaterials are being used in a wide range of scientific domains. Over the past thirty years, scientists have become interested in nanoscale medication delivery devices. As means of loading and delivering medications and vaccinations, they are extensively researched[7]. Excellent blood stability, a multipurpose nanocarrier design, and enhanced anticancer activity are further benefits[8-10].

Numerous substances produced from edible plants have been connected to cancer treatment and chemoprevention. Among these organic substances, naphthoquinones have demonstrated a number of pharmacological characteristics that make them potentially useful for the diagnosis and treatment of cancer[11,12]. Plumbagin (5-hydroxy2-methyl-1,4-naphthoquinone), the natural naphthoquinones found in *Plumbago zeylanica* roots, has recently been found to be an intriguing lead that exhibits a range of biological properties, such as antibacterial, anti-atherosclerotic, and anti-inflammatory. Furthermore, by blocking topoisomerse II, deactivating NF-kB, preventing tubulin binding from interrupting microtubule polymerization, and deactivating proto-oncogene Bcl-2, PBG hinders the growth of various cancer types[12]. Although PBG holds substantial medicinal promise, its clinical utility is hindered by a low oral bioavailability of 39%, stemming from its high lipid affinity and inadequate water solubility. Such factors present significant barriers to its effective formulation for therapeutic use. Moreover, achieving optimal therapeutic efficacy necessitates high or frequent dosing, which often leads to pronounced adverse effects. Thus, improving the solubility and anticancer impact of plumbagin will require a novel and effective technique[13,14].

Nanomedicine based drug delivery involves the use of several nanocarriers, with niosomes being one of the most effective. A vesicular nanoparticle known as a niosomes is made up of helper lipids like cholesterol and non-ionic surfactants that can make the bilayer stiffer. Niosomes possess a great deal of potential to specifically target tumor cells and exhibit a regulated release within them. Due to their remarkable attributes such as Uncomplicated fabrication, affordability, excellent stability, and the capability to encase both hydrophobic and hydrophilic drugs niosomes are considered a viable alternative to other delivery systems, especially liposomes[9].

2. Materials and Methods

2.1 Materials

Plumbagin powder was obtained from Yucca Enterprises Mumbai, cholesterol and span 60 was procured from Loba chemise, India. The MCF-7 cell lines were procured from the NCCS, Pune, India. The MTT reagent, dimethylsulfoxide, were procured from Sigma-Aldrich Chemical Private Ltd India.

2.2 Method of Preparation

Plumbagin-encapsulated niosomes were produced utilizing the reverse phase evaporation technology, as described in previous reports. Span 60 and cholesterol, in a 5:5 mole proportion, were dissolved in 10 ml of an organic solvent in a RBF. This was subsequent to introduction of 10 ml of a phosphate buffer (pH 7.4). Plumbagin was further added to the lipid mixture, and the two solutions were blended until a consistent emulsion formed. The resulting emulsion was transferred to a rotary evaporator (Labline PBV 7D, 100 rpm, 60°C) to slowly evaporate the organic solvent

under reduced pressure, resulting in the formation of a niosomes suspension. Finally, the formulation was sonicated for 10 minutes at 7°C (Labline LMUC-3) to make sure a consistent size range of the niosomal formulation. As per Table 1 different batch were formulated. This suspension is then allowed to freeze overnight at 20^0C refrigerator. To obtain powder, the frozen niosomes was then subjected to lyophilize. The formed niosomes was used for evaluated[15-19].

2.3 Characterization of Niosomes

2.3.1 Analysis of Particle Size, PDI and Zeta Potential

The particulate size, PDI, and zeta potential measured using the Horiba SZ 100, which employs dynamic light scattering technology. Prior to analysis, the formulations were diluted and transferred into a cuvette, where assessment were conducted at 25°C ± 5°C. Zeta potential was assessed using a specialized cuvette with an applied potential of 3.3 mV. For determining electrophoretic mobility, the niosomes formulations were placed in a zeta potential cuvette[20,21].

2.3.2 % Entrapment Efficiency

Entrapping efficiency represents the proportion of the drug encapsulated within the niosomes. The entrapment capability of the niosomal formulation was evaluated using a centrifugal methodology. Niosomes were isolated through ultracentrifugation at 18,000 rpm for 25 minutes, and the distinction between the total amount of drug that was collected inside the niosomes and the amount of not encapsulated active ingredient that was present in the supernatant was used to calculate the entrapment efficiency (%). The quantity of the free active ingredient in the supernatant was assessed spectrophotometrically with wavelength of 263 nm. The Entrapment Efficiency (EE) percentage was then derived as below[21].

Entrapment Efficiency (%) = (Total active ingredient–Free active ingredientin supernatant/ Total drug) ×100

2.3.3 FTIR Analysis

To assess the compatibility or potential interactions between plumbagin and other ingredients in the niosomal formulation, an FTIR analysis was conducted using a Bruker FTIR spectrophotometer. The samples for the investigation were prepared using the KBr pellet technique. In order to create a pellet that could be analyzed, 3 mg of the sample and 9 mg of KBr were blended together, and the mixture was then exposed to hydrostatic pressure at 8 Torr per square centimeter for one minute.

2.3.4 DSC Analysis

DSC was utilized to assess the thermal behavior and state of plumbagin, the physical mixture, and the optimized formulation. Samples with weight of 3-5 mg were placed in sample pans, and the testing was conducted within a thermal range of 25°C to 260°C at a thermal rate of 10°C per minute. The screening was executed in a nitrogen flow of 50 ml/min[22].

2.3.5 In Vitro Drug Release

An *in vitro* drug discharge investigation was executed to investigate the discharge pattern of free plumbagin and plumbagin-loaded niosomal formulation. The dialysis bag method was employed for this dissolution study. Separate dialysis bags, each containing either free plumbagin or lyophilized plumbagin-loaded optimized formulation equivalent to 10 mg of plumbagin, were phosphate buffer-soaked for the entire night (pH 7.4). After both ends were sealed the bags, they were connected to the paddles of a dissolution test instrument containing 900 ml of phosphate buffer (pH 7.4). The whole system was maintained at 37 ± 0.5 °C with a turning around speed of 100 rpm. At predefined time range, samples were taken out and substituted with a same volume of newly prepared medium to preserve sink conditions. The quantity of active ingredient released from the formulation was computed using a UV instrument at 263 nm[23,24].

2.3.6 Kinetic Release Study

The *in vitro* drug discharge data were assessed utilizing various kinetic models. The release kinetics of plumbagin from the niosomes was computed through multiple models, including zero-order, first-order, Higuchi, and Korsmeyer-Peppas (KP) simulations.

$Q_t = Q_0 + k_0 t$

$Q_t = Q_0 e^{-k1t}$ k1/2.303

$Q_t = k_H . t^{1/2}$

$M_t/M = k_p t^n$

In these models, Q_t represents the cumulative amount of active ingredient discharge at time t, M_t/M denotes the fraction of active ingredient discharge, and the constants k_0, k_1, k_H and k_p correspond to the 0-order, 1st-order, Higuchi, and Korsmeyer-Peppas models, respectively. Also Q_0 is the quantity of the encapsulated active ingredient, and n is the diffusional exponent. The determination coefficient (r^2) for each model was computed to figure out the system that best fits the discharge data[25-27].

2.4 *In Vitro* Cytotoxicity (MTT Assay) for Anticancer Activity

2.4.1 Preparation of Cells

MCF-7 colonies were cultivated in MEM with Non-Essential Amino Acids (NEAA) and fortified with 10% (v/v) bovine serum. The colonies were retained at 37°C in a 5% CO_2 condition, with the complete medium being replaced every 2 to 3 days.

2.4.2 MTT Assay Procedure

The cytotoxic impact of the niosomes formulation were assessed using the MTT assay with MCF-7 breast cancerous cells. The MCF-7 cell line, sourced from NCCS, Pune, India, was grown in 96-well plates and humidified incubator with 5% CO_2 for 24 hours, achieving a near-confluent monolayer. Following the removing of the growth media, cells were exposed to seven distinct concentrations of plumbagin and plumbagin-loaded niosomes (10, 25, 50, 100, 250, 500, and 1000 µg/ml). Cisplatin was used as a reference standard. Cells cultured without any test substances served as the control. Following a 24 hours incubation and 5% CO_2, cells were inspected under an inverted microscope for any morphological changes or signs of cell death. After this observation, the medium was substituted with 100 µl of newly prepared medium and 10 µl of MTT dye. The plates were then maintained for 4 hours at 37°C with 5% carbon dioxide. Upon, 100 µl of a solubilizing solution was introduced to wells, and the plates were left at 37°C with 5% CO_2 for an extra hour. Absorbance of the formazan crystals was quantified at 570 nm with the help of a microplate reader to determine cell survival percentage, calculated according to established formulas[28-34].

Percent Cell Survival (%) = (Absorbance of Test/ Absorbance of Control) * 100

3. Result and Discussion

The characterization of formulated niosomes of plumbagin were studied and results are discussed below.

3.1 Analysis of Particle Size, PDI and Zeta Potential

The optimization of niosomal formulations was achieved by adjusting the molar ratio of surface active agent to cholesterol to maximize entrapment efficiency, target particulate size, zeta potential, and PDI. The span 60 to cholesterol ratio was refined to identify the optimal formulation. Particle size measurements, conducted using dynamic light scattering with a Horiba SZ 100, ranged from 84.5 ± 5.85 nm to 123.5 ± 4.82 nm (Figure 1). An increase in particle size was noted with higher concentrations of cholesterol and span 60, likely due to the development of a more robust bilayer membrane. Formulation homogeneity was assessed using the PDI, with values below 0.1 demonstrating high homogeneity and values over 0.3 suggesting significant heterogeneity. The optimized formulation (FC9) had a PDI of 0.143 ± 0.067, indicating satisfactory uniformity and sturdiness. The stability of the niosomes formulations was evaluated based on zeta potential. Typically, a zeta potential close to ±30 mV ensures stability for longer duration. The optimized batch exhibited a zeta potential of -26.8 ± 2.13 mV shown in Figure 2. High negative zeta potential values generally reflect stable formulations and minimize aggregation. The inclusion of plumbagin in niosomes resulted in lower zeta potential values, contributing to increased formulation stability.

3.2 Determination of % Entrapment Efficiency (EE)

The entrapment efficiency data across various formulation codes (FC1 to FC9) indicate that FC9 stands out as the optimized formulation, achieving the highest entrapment efficiency, result given in table no 1. The % EE for the optimized FC9 was measured at 91.42 ± 2.19 %. This high drug loading is advantageous for systemic administration, ensuring a substantial release of plumbagin at the intended site of action. In comparison, Barani *et al*., reported a loading efficiency of 69% for lawsone-encapsulated niosomes with a

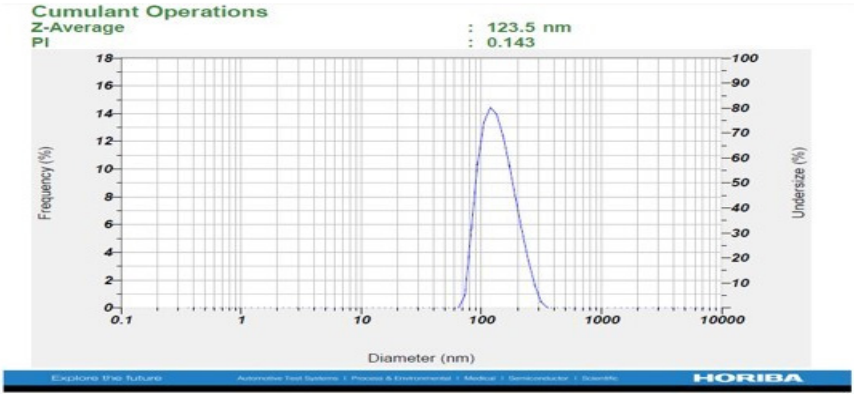


Figure 1. Particle size of FC9 formulation.

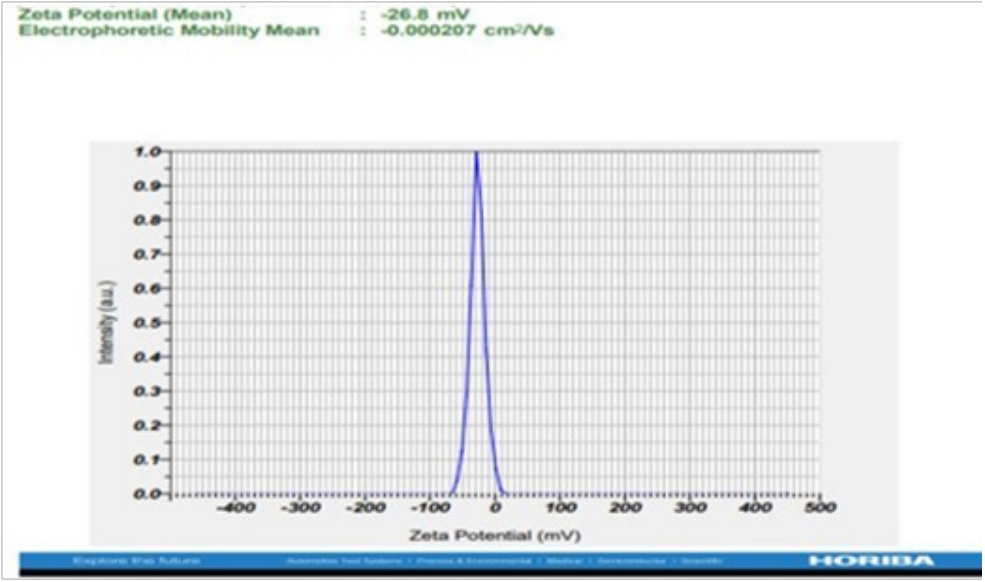


Figure 2. Zeta potential of FC 9 formulation.

particulate size of 0.3 microns. The Plumbagin-loaded niosomes developed in this study not only demonstrate superior loading efficiency but also exhibit a reduced particle size relative to the sizes reported earlier by Barani *et al*[21].

3.3 FTIR Analysis

The FTIR spectra for cholesterol, span 60, Plumbagin, its physical mixture, and the optimized batch (FC9) are illustrated in Figures 3a, 3b, 3c, 3d, and 3e, respectively. In the significant peak of plumbagin, appearance of strong intensity bands 3733.50 cm^{-1} represents -OH group, strong firm band at 1644.98 cm^{-1} represents ketone group and firm band at 2995.02 cm^{-1} represents alkyl -CH group (Figure 3c). FT-IR of physical mixture exhibit intense band at 3442.31 cm^{-1} represents -OH group, strong intense band at 1645.95 cm^{-1} represents ketone group, medium intense band at 1744.3 cm^{-1} represents ester C=O group, strong intense band at 2963.09 cm^{-1} represents alkene =CH group and intense band at 2845.45 cm^{-1} represents alkyl -CH group. FTIR spectra physical mixture also had shown all significant peak of plumbagin (Figure 3d). The optimized batch (FC9) exhibit strong intense band at 3425.12 cm^{-1} represent-OH group, 1641.66 cm^{-1} represent ketone C=O group, 1734.37 cm^{-1} represent ester C=O group,

Table 1. Optimization on the basis of surfactant and cholesterol

Sr. No.	Formulation Code	Span 60: Cholesterol; Plumbagin (% w/w/w)	Average Particulate Size (nm)	PDI	Zeta Potential (mV)	EE (%)
1.	FC1	1:1:1	84.5± 5.85	0.321 ± 0.057	-18.4± 1.65	34.60 ± 0.97
2.	FC2	2:1:1	92.4 ± 9.25	0.318 ± 0.08	-19.2 ± 1.82	42.4 ± 1.27
3.	FC3	3:1:1	95.5± 9.59	0.364 ± 0.09	-21.6 ± 1.24	46.4 ± 1.82
4.	FC4	4:1:1	117.6± 7.24	0.214 ± 0.06	-26.7 ± 1.16	48.7 ± 2.37
5.	FC5	5:1:1	91.45± 6.81	0.256 ± 0.057	-29.87± 1.83	57.63 ± 2.16
6.	FC6	5:2:1	101.6± 4.52	0.097 ± 0.08	-31.4 ± 2.31	64.51 ± 3.12
7.	FC7	5:3:1	110.9± 4.98	0.125 ± 0.11	-35.47 ± 2.54	74.62 ± 2.83
8.	FC8	5:4:1	119.58± 7.24	0.208 ± 0.09	-33.13 ± 2.18	84.65 ± 2.87
9.	FC9	5:5:1	123.5± 4.82	0.143 ± 0.067	-26.8 ± 2.13	91.42 ± 2.19

3027.64 cm^{-1} represent alkene =CH group, 2923.90 cm^{-1} represent alkyl -CH group (Figure 3e). The IR spectrum displayed distinct peaks corresponding to the vibrations of key functional groups at specific wave numbers. All characteristics peaks were seen in the optimized formulation ensured that no new peaks were observed. This shown that plumbagin was compatible with vesicle components and no new chemical interaction happens between them.

3.4 DSC Analysis

The DSC thermogram technique utilized to confirm the physical state of niosomes formulation. The DSC thermogram of plumbagin, its mixture and optimized batch Plumbagin niosomes (FC9) was recorded and displayed in Figures 4a, 4b and 4c respectively. In the DSC analysis of plumbagin alone, a significant endothermic peak noticed at 79.61°C, indicating its high purity (Figure 4a). In the physical mixture unique endothermic peaks of the individual components were evident (Figure 4b). The DSC analysis of the optimized lyophilized batch (Figure 4c) revealed a mannitol peak at 111.61°C. It was also observed that the thermogram showed no additional peaks of available free plumbagin, indicating that there had not been any precipitation and that the plumbagin had been completely encapsulated in the vesicles. It follows that cholesterol and span 60 merge, and this observation confirmed the formation of plumbagin niosomes and the lack of the predicted plumbagin leakage[22].

3.5 *In vitro* Release Study

Figure 5 displays the *in vitro* discharge profiles for both free plumbagin and plumbagin niosomes. A notable difference was observed in the cumulative percentage release between the free plumbagin and the plumbagin niosomes formulation, with the latter exhibiting a slower active ingredient release rate compared to the solution of plumbagin. The release of plumbagin from niosomes followed a biphasic pattern: An initial rapid discharge phase occurring over 1 to 6 hours, followed by a prolonged, steady discharge phase from 9 to 24 hours. This biphasic release profile is typical of bilayer vesicles. Research has indicated that the regulated and prolonged discharge of drugs from niosomes is a crucial factor in effective cancer treatment[20,21]. Timmadonu *et al.* developed paclitaxel-encapsulated niosomes and assessed their release kinetics. Their formulation achieved a 95.6% drug release after 17 hours[23]. In different study, Jain *et al.* developed nanoparticles encapsulating duloxetine HCl, with approximately 12% of the therapeutic agent being released 2 hours later[24]. The above mentioned research studies shown that, drug encapsulated niosomes shows sustained release pattern.

3.6 Kinetic Release Study

The drug discharge profiles were assesd utilizing Zero-order, First-order, Higuchi, and Korsmeyer-peppas simulations. Table 2 indicates that the Higuchi model finely matched the experiment findings, as determined by the correlation coefficient ($R^2 > 0.97$)[25].

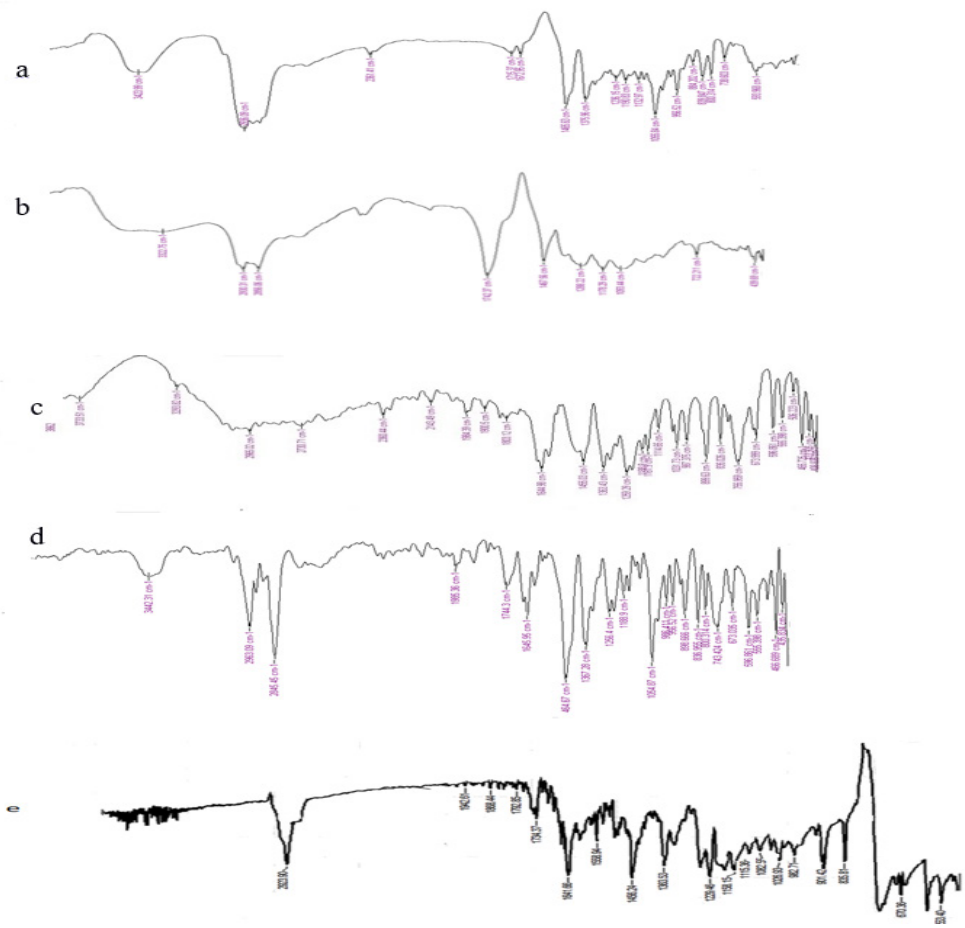


Figure 3. FTIR spectrum; **(a).** Cholesterol; **(b).** Span 60; **(c).** Plumbagin; **(d).** Physical mixture; **(e).** Plumbagin niosomes.

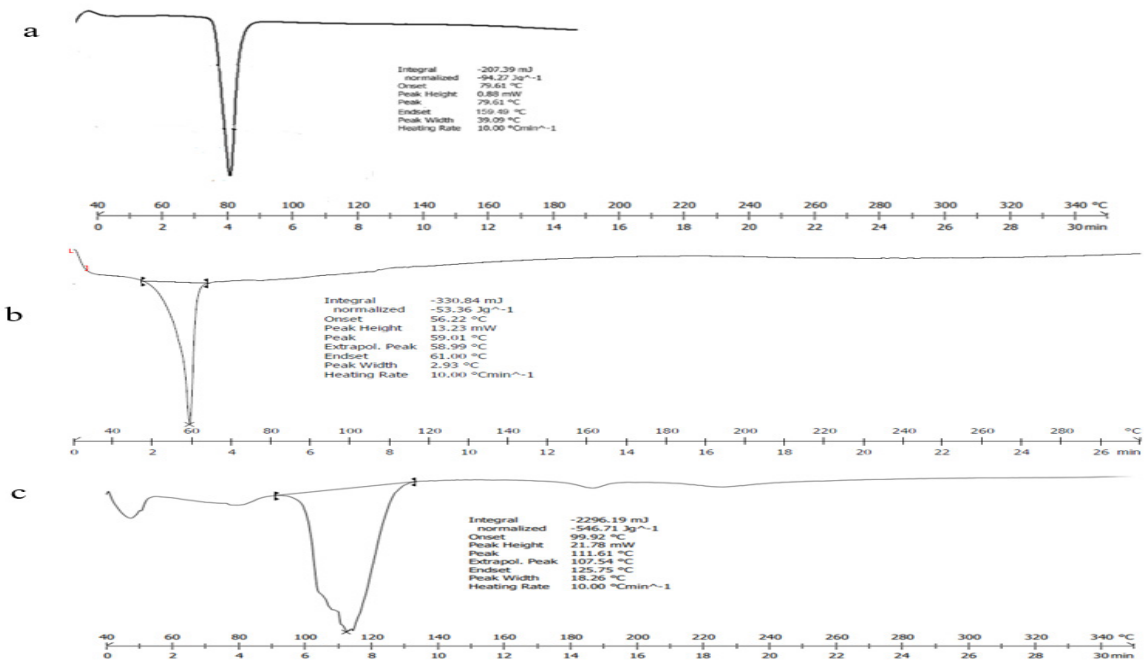


Figure 4. DSC thermogram of **(a)** plumbagin **(b)** physical mixture **(c)** plumbagin niosomes formulation.

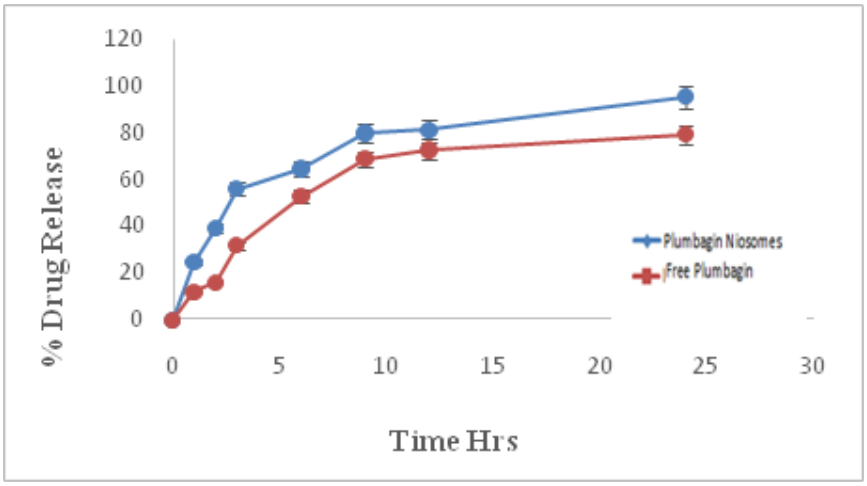


Figure 5. *In vitro* release profiles of free plumbagin and plumbagin niosomesin PBS 7.4 at 37°C.

Table 2. Model, equation, and regressions of plumbagin discharge from niosomes

Model	Equation	R^2
Zero-order	y = 3.3678x + 31.062	R^2 = 0.6999
First order	y = 19.983x + 10.2	R^2 = 0.9242
Higuchi	y = -0.0526x + 1.8883	R^2 = 0.971
Kors-peppas	y = 0.0457x + 1.2158	R^2 = 0.3128

3.7 *In Vitro* Cytotoxicity (MTT Assay) for Anticancer Activity

This research investigated the anticancer efficacy of free plumbagin versus plumbagin encapsulated in niosomes opposite to the MCF-7 cell line. To identify the optimal concentration, we evaluated various concentrations of free plumbagin, plumbagin niosomes, and cisplatin (ranging from 10 to 1000 µg/ml) using the MTT assay over 24 hours. The relationship between drug concentration and toxicity is illustrated in Figure 6. For comparative purposes, we focused on a concentration of 250 µg/ml. The outcome displayed that plumbagin-entrapped niosomes demonstrated greater cytotoxicity compared to free plumbagin. Specifically, at 250 µg/ml, the cell survival rates were 87.57% for cisplatin and 43.82% for free plumbagin, while plumbagin niosomes had a cell survival rate of just 15.25%. Optical microscopic analysis of cell proliferation in control and plumbagin-loaded niosomes-treated samples, as shown in Figure 7, corroborates these findings. Control cells spread evenly across the substrate, while at higher drug concentrations, the cells adopted a more spherical shape and exhibited reduced spreading.

4. Conclusion

The potential of plumbagin-loaded niosomes as efficient nanocarriers for targeted cancer medication delivery is demonstrated by this work. The niosomes demonstrated a mean particle size between 84.5 ± 5.85 nm and 123.5 ± 4.82 nm, with particle size increasing as the surfactant and cholesterol molar ratios were raised. The optimized batch (FC9) had a zeta potential of -26.8 ± 2.13 mV and 91.42 ± 2.19 % entrapment efficiency. *In vitro* release experiments demonstrated a prolonged release profile for the niosomes in contrast to free plumbagin. Moreover, the MTT assay indicated that plumbagin-loaded niosomes at 250 µg/ml with a notable cytotoxic action on the MCF-7 cells, with a cell viability rate of 15.25%, whereas free plumbagin had a higher survival rate of 43.82%. These findings suggest that niosomes-encapsulated plumbagin is a highly effective nanocarrier for enhancing cancer therapy, demonstrating substantial promise in drug delivery applications.

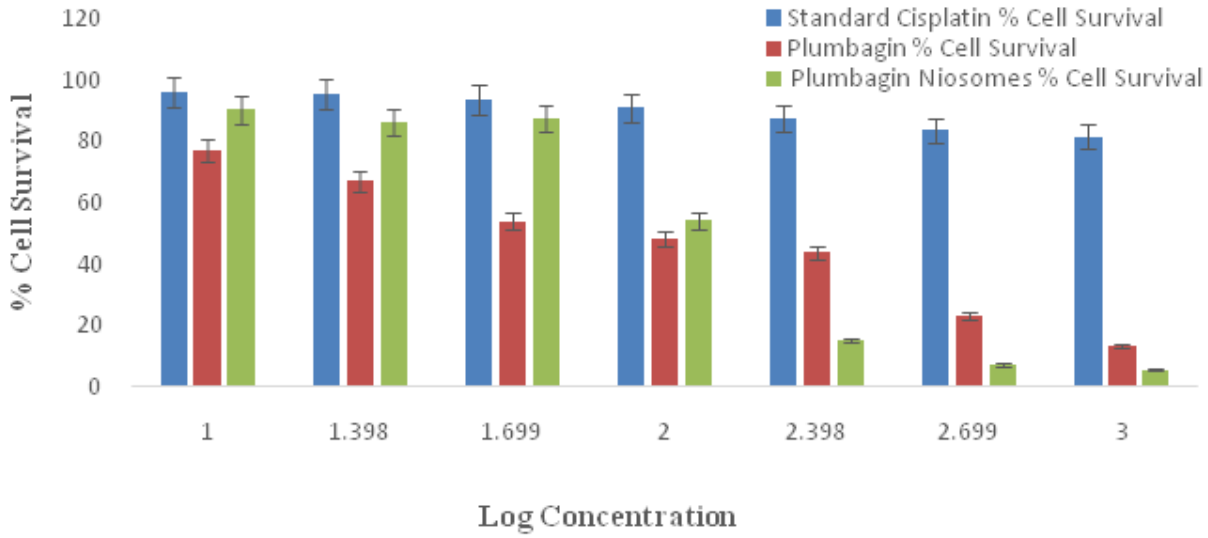


Figure 6. The bar graph indicating % cell survival of standard cisplatin, free plumbagin and plumbagin niosomes formulation against MCF-7 cell line.

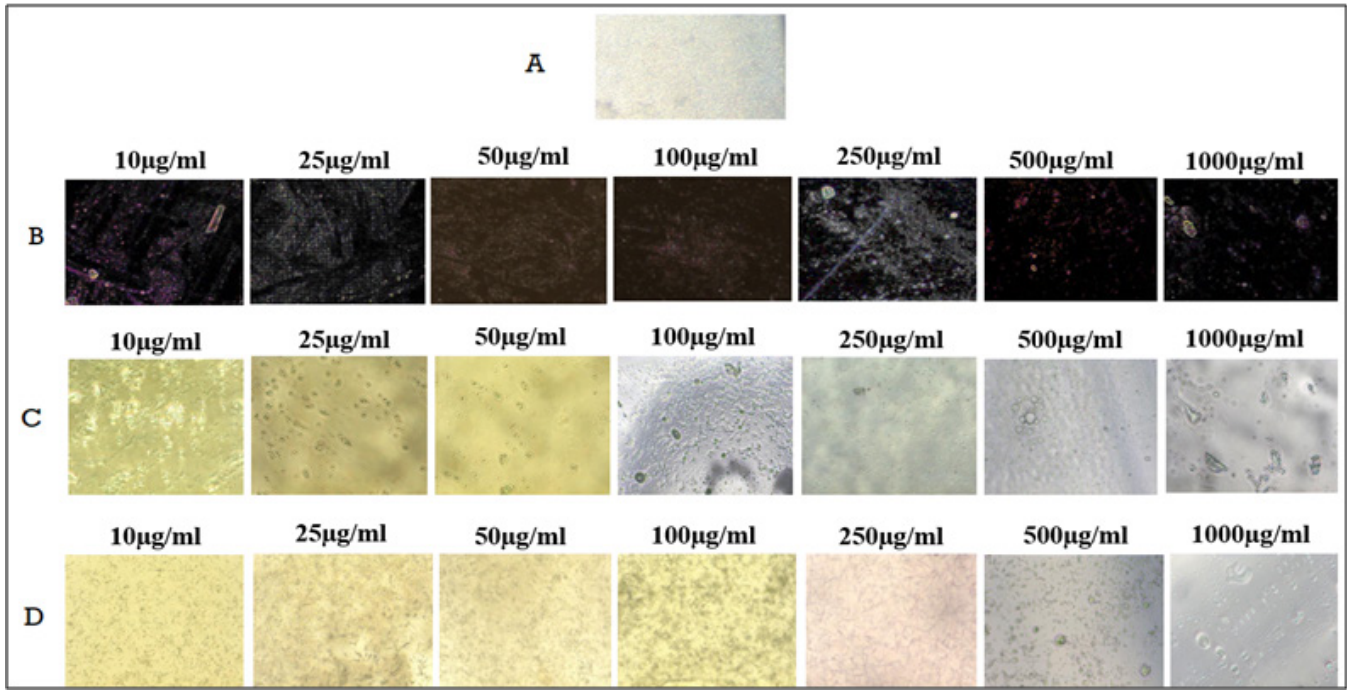


Figure 7. Morphological changes of cytotoxicity against MCF-7 cell line; (**A**). Control cell; **(B).** Cisplatin standard; **(C).** Plumbagin; **(D)**. Plumbagin niosomes.

5. Acknowledgement

The researchers would want to convey their profound gratitude to PES Modern College of Pharmacy, Moshi, Pune, for providing the necessary laboratory facilities required for this research. We also extend our gratitude to the college library for granting access to essential e-resources. We are deeply grateful for the college's support throughout every stage of this work. The findings presented in this paper are part of an academic thesis.

6. Authors Contributions

Jyoti Jawale: Whole research work was conducted; Vrushali Kashikar: Reviewed the results and approved the final version of the manuscript; Shashikant Dhole: Reviewed the results and approved the final version of the manuscript; Sonali Devne: Analyzed Data and discussed result. All authors have read and agreed to the published version of the manuscript.

7. References

1. Bharali DJ, Mousa SA. Emerging nanomedicines for early cancer detection and improved treatment: Current perspective and future promise. Pharm Therap. 2010; 128(2):324-335. https://doi.org/10.1016/j.pharmthera.2010.07.007
2. Zhao G, Zhang L, Sun K. Capacitive contribution to lithium storage capacity in porous MoO3 films. J Electroanal Chem. 2013; 694:61-67. https://doi.org/10.1016/j.jelechem.2013.02.005
3. Luo Y, Prestwich G. Cancer-targeted polymeric drugs. Curr Cancer Drug Targets. 2002; 2(3):209-226. https://doi.org/10.2174/1568009023333836
4. Sutradhar KB, Amin ML. Nanotechnology in cancer drug delivery and selective targeting. ISRN Nanotechnology. 2014. https://doi.org/10.1155/2014/939378
5. Tannock IF, Lee CM, Tunggal JK, Cowan DS, Egorin MJ. Limited penetration of anticancer drugs through tumor tissue: A potential cause of resistance of solid tumors to chemotherapy. Clin Cancer Res. 2002; 8(3):878-884. PMID: 11895922
6. Chakraborty M, Jain S, Rani V. Nanotechnology: Emerging tool for diagnostics and therapeutics. Appl Biochem Biotechnol. 2011; 165:1178-1187. https://doi.org/10.1007/s12010-011-9336-6
7. Shah MR, Imran M, Ullah S. Lipid-based nanocarriers for drug delivery and diagnosis. William Andrew. 2017.
8. Jin SE, Jin HE, Hong SS. Targeted delivery system of nanobiomaterials in anticancer therapy: From cells to clinics. Biomed Res Int. 2014. https://doi.org/10.1155/2014/814208
9. Sakpakdeejaroen I, Somani S, Laskar P, Mullin M, Dufes C. Transferrin-bearing liposomes entrapping plumbagin for targeted cancer therapy. J Interdiscip Nanomed. 2019; 4(2):54-71. https://doi.org/10.1002/jin2.56
10. Jeetah R, Bhaw-Luximon A, Jhurry D. Nanopharmaceutics: Phytochemical-based controlled or sustained drug-delivery systems for cancer treatment. J Biomed Nanotechnol. 2014; 10(9):1810-1840. https://doi.org/10.1166/jbn.2014.1884
11. Rizwanullah M, Amin S, Mir SR, Fakhri KU, Rizvi MMA. Phytochemical based nanomedicines against cancer: Current status and future prospects. J Drug Target. 2018; 26(9):731-752. https://doi.org/10.1080/1061186x.2017.1408115
12. Yin Z, Zhang J, Chen L, Guo Q, Yang B, Zhang W, Kang W. Anticancer effects and mechanisms of action of plumbagin: Review of research advances. Biomed Res Int. 2020. https://doi.org/10.1155/2020/6940953
13. Bothiraja C, Kapare HS, Pawar AP, Shaikh KS. Development of plumbagin-loaded phospholipid-Tween® 80 mixed micelles: Formulation, optimization, effect on breast cancer cells and human blood or serum compatibility testing. Ther Deliv. 2013; 4(10):1247-159. https://doi.org/10.4155/tde.13.92
14. Bothiraja C, Pawar AP, Mali AJ, Shaikh KS. Improved pharmaceutical properties of surface modified bioactive plumbagin crystals. Int J Surf Sci Eng. 2013; 7(2):181-195. https://doi.org/10.1504/ijsurfse.2013.053708
15. Junyaprasert VB, Singhsa P, Jintapattanakit A. Influence of chemical penetration enhancers on skin permeability of ellagic acid-loaded niosomes. Asian J Pharm Sci. 2013; 8(2):110-117. https://doi.org/10.1016/j.ajps.2013.07.014
16. Junyaprasert VB, Teeranachaideekul V, Supaperm T. Effect of charged and non-ionic membrane additives on physicochemical properties and stability of niosomes. AAPS Pharm Sci Tech. 2008; 9:851-859. https://doi.org/10.1208/s12249-008-9121-1
17. Bendas ER, Abdullah H, El-Komy MHM, Kassem MAA. Hydroxychloroquine niosomes: A new trend in topical management of oral lichen planus. Int J Pharm. 2013; 458(2):287-295. https://doi.org/10.1016/j.ijpharm.2013.10.042
18. Mavaddati MA, Moztarzadeh F, Baghbani F. Effect of formulation and processing variables on dexamethasone entrapment and release of niosomes. J Clust Sci. 2015; 26:2065-2078. https://doi.org/10.1007/s10876-015-0908-4
19. Sankhyan A, Pawar PK. Metformin loaded non-ionic surfactant vesicles: Optimization of formulation, effect of process variables and characterization. DARU J Pharm Sci. 2013; 21:1-8. https://doi.org/10.1186/2008-2231-21-7
20. Hajizadeh MR, Parvaz N, Barani M, Khoshdel A, Fahmidehkar MA, Mahmoodi M, Torkzadeh-Mahani M. Diosgenin-loaded niosome as an effective phytochemical nanocarrier: Physicochemical characterization, loading efficiency, and cytotoxicity assay. DARU J Pharm Sci. 2019; 27:329-339. https://doi.org/10.1007/s40199-019-00277-0
21. Barani M, Mirzaei M, Torkzadeh-Mahani M, Nematollahi MH. Lawsone-loaded niosome and its antitumor activity in MCF-7 breast cancer cell line: A nano-herbal treatment for cancer. DARU J Pharm Sci. 2018; 26:11-17. https://doi.org/10.1007/s40199-018-0207-3
22. Tyagi R, Waheed A, Kumar N, Ahad A, Bin Jardan YA, Mujeeb M, Kumar A, Naved T, Madan S. Formulation

and evaluation of plumbagin-loaded niosomes for an antidiabetic study: Optimization and *in vitro* evaluation. Pharm. 2023; 16(8):1169. https://doi.org/10.3390/ph16081169

23. Suriyaprakash TNK, Parthiban S, Prabu SL, Sumathi A. Formulation and evaluation of paclitaxel niosome for its improved anti-cancer activity. Acta Pharm Sci. 2011; 53(3).
24. Jain R, Sukla SK, Nema N, Panday A. Drug nano-particle: A release kinetics. J Nanomed Nanotechnol. 2015; 6(5):1-6. https://doi.org/10.4172/2157-7439.1000317
25. Katrolia A, Chauhan SB, Shukla VK. Formulation and evaluation of metformin hydrochloride-loaded curcumin-lycopene niosomes. SN Appl Sci. 2019; 1:1-6. https://doi.org/10.1007/s42452-019-1768-6
26. Negi P, Madhur Aggarwal M, Sharma G, Rathore C, Sharma G, Singh B, Katare OP. Niosome-based hydrogel of resveratrol for topical applications: An effective therapy for pain related disorder (s). Biomed Pharmacother. 2017; 88:480-487. https://doi.org/10.1016/j.biopha.2017.01.083
27. Khan DH, Bashir S, Khan MI, Figueiredo P, Santos HA, Peltonen L. Formulation optimization and *in vitro* characterization of rifampicin and ceftriaxone dual drug loaded niosomes with high energy probe sonication technique. J Drug Deliv Sci Tech. 2020; 58:101763. https://doi.org/10.1016/j.jddst.2020.101763
28. Graidist P, Martla M, Sukpondma Y. Cytotoxic activity of *Piper cubeba* extract in breast cancer cell lines. Nutr. 2015; 7(4):2707-2718. https://doi.org/10.3390/nu7042707
29. Riss TL, Moravec RA, Niles AL, Duellman S, Benink HA, Worzella TJ, Minor L. Cell viability assays. Assay Guidance Manual. 2016.
30. Meerloo JV, Kaspers GJL, Cloos J. Cell sensitivity assays: The MTT assay. Cancer Cell Culture: Methods and Protocols. Humana Press Inc. 2011:237-245. https://doi.org/10.1007/978-1-61779-080-5_20
31. Kumar S, Baldi A, Sharma DK. *In vitro* antioxidant assay guided *ex vivo* investigation of cytotoxic effect of phytosomes assimilating taxifolin rich fraction of *Cedrus deodara* bark extract on human breast cancer cell lines (MCF7). J Drug Deliv Sci Tech. 2021; 63:102486. https://doi.org/10.1016/j.jddst.2021.102486
32. Malaiyandi J, Anandapadmanaban G, Perumalsamy H, Kilankajae A, Chellappan DK, Dua K, Girija S, Balusamy SR. Corrigendum to "Plumbagin from two *Plumbago* species inhibits the growth of stomach and breast cancer cell lines. Ind Crop Prod. 2020; 149:112332. https://doi.org/10.1016/j.indcrop.2020.112332
33. Han W, Wang S, Liang R, Wang L, Chen M, Li H, Wang Y. Non-ionic surfactant vesicles simultaneously enhance antitumor activity and reduce the toxicity of cantharidin. Int J Nanomedicine. 2013; 8(1):2187-2196. https://doi.org/10.2147/ijn.s43568
34. Xu YQ, Chen WR, Tsosie JK, Xie X, Li P, Wan JB, He CW, Chen MW. Niosome encapsulation of curcumin: Characterization and cytotoxic effect on ovarian cancer cells. J Nanomater. 2016. https://doi.org/10.1155/2016/6365295